Acta Crystallographica Section A
Foundations of Crystallography
ISSN 0108-7673

Received 13 March 2002
Accepted 15 April 2002

The Goos–Hänchen effect at Bragg diffraction

Kenji Tamasaku* and Tetsuya Ishikawa

RIKEN Harima Institute/SPring-8, Mikazuki, Hyogo 679-5148, Japan. Correspondence e-mail: tamasaku@postman.riken.go.jp

The strong incident-angle dependence of the phase of complex reflectivity causes a shift of the reflected beam from the geometrically expected path. This effect, known as the Goos–Hänchen effect in the visible region, was observed for Bragg-case diffraction in the hard X-ray region. The shift was found to be in good agreement with the theory.

1. Introduction

Most dynamical theories of X-ray diffraction assume ideal incident waves, such as a monochromatic plane wave or a monochromatic spherical wave. However, real X-rays have finite spread in both space and time. A bounded beam is regarded as a coherent superposition of plane waves which have slightly different wave vectors. When a bounded beam impinges on a perfect crystal, each one of these plane waves will be diffracted with a slightly different phase depending on the incident angle and the wavelength. Such a phase dependence will cause deviations from geometrical optics. Suppose that the beam is bounded spatially and that the angular divergence is much smaller than the rocking-curve width of the relevant diffraction (spectrally narrow beam condition), the diffracted beam will be shifted laterally from the geometric path (Andreev *et al.*, 1987; Berenson, 1989), which is the X-ray analog of the Goos–Hänchen effect (Goos & Hänchen, 1947).

In this short note, we will report an experimental observation of the Goos–Hänchen effect for dynamical X-ray diffraction in the Bragg geometry.

2. Experimental

The experiment was performed on an undulator beamline for coherent X-ray optics (BL29XUL) at SPring-8 (Tamasaku *et al.*, 2001). To obtain a spectrally narrow beam in the angular domain, two asymmetrically cut Si 220 crystals were used for a collimator. These have asymmetric angles of 9.5 and 9.0°, and asymmetric factors of $1/b = 43.2$ and 19.7 at the wavelength of the experiment, $\lambda = 0.663$ Å. The vertical angular divergence of the undulator radiation, which was estimated to be 3.1″ (FWHM), was reduced down to 0.004″ (FWHM) by the collimator. A slit with a vertical aperture of $a = 1.0$ mm limited the spatial extent of the beam incident on the sample. The beam after the slit had a uniform intensity profile along the vertical direction and a diffraction limited angular divergence of $\lambda/a \sim 0.014''$. The sample was a symmetric Si 220 crystal in the Bragg geometry. The angular acceptance of the sample was estimated to be $\omega = 2.02''$. The angular divergence of the incident beam was much smaller than the acceptance of the sample, and satisfied the condition of the spectrally narrow beam. All crystals were arranged non-dispersively and had vertical scattering planes in order that the incident beam became σ polarized.

To observe the Goos–Hänchen shift, we measured the edge positions of the diffracted beam from the sample along the scattering plane. Both edges on the head side and the tail side were measured at 26 different incident angles with 0.2″ steps. The shape of the beam edge was measured by knife-edge scan. First the intensity after the knife edge was recorded as a function of the knife-edge position, which was measured going towards the tail side. Then the intensity was differentiated with respect to the knife-edge position to give the intensity profile of the diffracted beam. The beam edge was determined by the position giving half of the intensity at the top flat region. The knife edge was mounted on a translational stage which was scanned parallel to the sample surface by 1 μm steps. The resolution and the reproducibility of the translational stage was 0.25 μm and less than 0.5 μm, respectively. The intensity after the knife edge was measured by a PIN diode to achieve higher signal-to-noise ratio. An ionization chamber monitored the reflected intensity before the knife edge to normalize the output signal from the PIN diode.

3. Results and discussions

Fig. 1 shows the intensity map along the scattering plane on both the head side and the tail side as a function of the deviation from the Bragg angle, $\Delta\theta$. Note that the intensity was measured along the sample surface. The beam position measured at the knife edge shifts geometrically by $2\Delta\theta L/\sin\theta_B$ along the translation direction of the

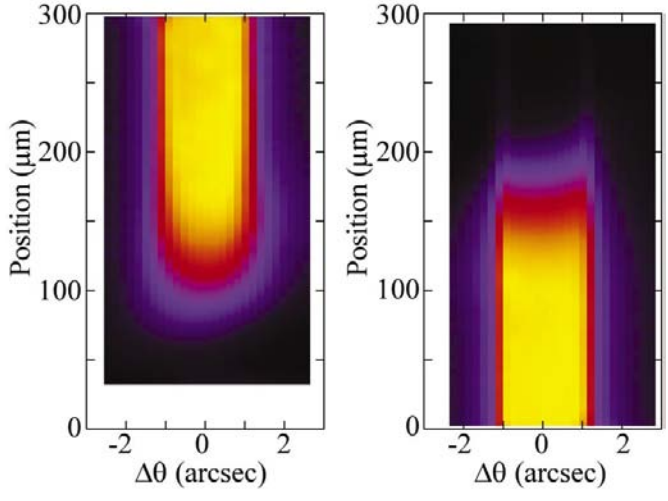

Figure 1
Intensity profile of the diffracted beam section along the sample surface at the different incident angles, $\Delta\theta$. The head side edge (left panel) and the tail side edge (right panel) are shown. The yellow parts indicate stronger intensity.

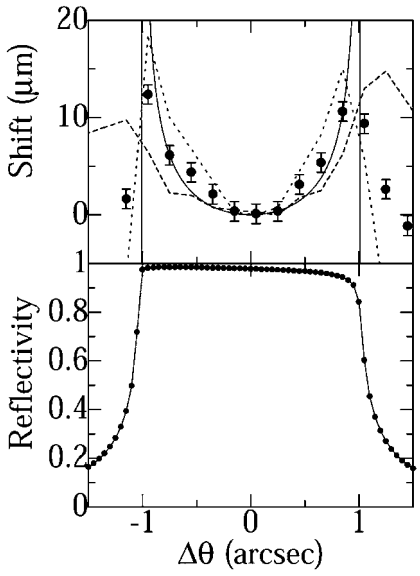

Figure 2
Rocking curve of sample (lower panel) and relative shifts of the head side edge (dotted line), of the tail side edge (broken line) and of the beam center (closed circles) as a function of the incident angle, $\Delta\theta$ (upper panel). The solid line is the theoretical prediction without absorption.

knife edge, corresponding to the variation of the scattering angle. Here L is the distance from the sample to the knife edge and θ_B is the Bragg angle, respectively. This unimportant geometrical displacement was subtracted from the raw data. The beam edges on both sides shifted towards the tail side at the incident angles near the edges of the diffraction. A weak tailing illumination was observed on the tail side at each edge of the diffraction ($\Delta\theta \simeq \pm 1''$). The widths of the beam edges were broadened compared to that of the incident beam. For example, the edge widths at the Bragg angle ($\Delta\theta = 0''$) were about 70 μm (10–90% width) along the surface, which corresponds to 12 μm along the beam cross section. On the other hand, the incident beam had a sharper edge, about 4 μm along the beam cross section. The dull edges may be due to diffraction at the slit.

The relative shift of the beam center is plotted in Fig. 2 together with the edge shift on both sides. The beam center was determined as a middle point of the two edges. Each shift was measured relative to the position at $\Delta\theta \simeq 0''$. The lateral shift of the diffracted beam center increases as the incident angle approaches the edge of diffraction. The theoretical shift along the sample surface, d (Andreev *et al.*, 1987; Berenson, 1989), is plotted in Fig. 2 using

$$d = \Delta_0/(1 - W^2)^{1/2} \qquad (1)$$

for $|W| < 1$. Here $\Delta_0 = 2\cos\theta_B/(kC|\chi_g|)$, $k = 2\pi/\lambda$, $C = 1$ (σ polarization) or $C = \cos(2\theta_B)$ (π polarization), χ_g is the gth Fourier coefficient of the electric polarizability, $W = 2\Delta\theta/\omega$ is the normalized angular deviation from θ_B. Δ_0 is estimated to be 12.5 μm using $|\chi_g| = 1.67 \times 10^{-6}$ for Si 220 (Sasaki, 1984). The $\Delta\theta$ dependence of the shift is in good agreement with (1) within the range of total reflection. At the edges of diffraction, $|W| = 1$, (1) diverges and is no longer valid. Berenson (1989) calculated analytically the shift at $|W| = 1$ for a Gaussian beam [*cf.* equation (45) in his paper]. The shift at the edges in the present case is estimated to be 97 μm from the geometric path, which is much larger than the experimental observation. The discrepancy may be accounted for by absorption which is ignored in the calculation. The broader peak of the shift at $\Delta\theta = 1''$ than at $\Delta\theta = -1''$ may be related to the stronger dynamical absorption at higher glancing angles.

The lateral shift was calculated using the complex reflectivity (Andreev *et al.*, 1987; Berenson, 1989). We would like to point out that the lateral shift is closely related to the extinction effect. The imaginary part of the perpendicular component of the wavevector to the surface is given by $k_z^i = \pi(1 - W^2)^{1/2}/(\Lambda\tan\theta_B)$, where $\Lambda = \lambda\cos\theta_B/(C|\chi_g|)$ is the *Pendellösung* distance (Authier, 2001). Using k_z^i, (1) is rewritten as

$$d = \frac{1}{k_z^i \tan\theta_B} = \frac{2l_B}{\tan\theta_B}. \qquad (2)$$

Here $l_B = 1/(2k_z^i)$ is nothing but the extinction distance in Bragg-case diffraction.

4. Conclusions

We have observed the Goos–Hänchen effect at the Bragg diffraction in good agreement with the theory. Because the lateral shift is related to the extinction effect, it will cause a time delay of the diffracted beam, which depends on the incident angle. The tailing illumination should be delayed more, since it is originating from the beam penetrating deeper. Full understanding of the diffraction of the bounded beam may require further theoretical study in both space and time, and will be necessary when well collimated and short pulsed X-rays from a free electron laser will be available.

References

Andreev, A. V., Gorshkov, V. E. & Il'inskii, Yu. A. (1987). *Zh. Tekh. Fiz.* **57**, 511–522; Engl. transl: *Sov. Phys. Tech. Phys.* (1987). **32**, 308–314.
Authier, A. (2001). *Dynamical Theory of X-ray Diffraction*, p. 133. Oxford University Press.
Berenson, R. (1989). *Phys. Rev. B*, **40**, 20–28.
Goos, F. & Hänchen, H. (1947). *Ann. Phys. (Stuttgart)*, **1**, 333–346.
Sasaki, S. (1984). *Anomalous Scattering Factors for Synchrotron Radiation Users, Calculated Using Cromer and Liberman's Method.* KEK Report 83-22. National Laboratory for High Energy Physics, Japan.
Tamasaku, K., Tanaka, Y., Yabashi, M., Yamazaki, H., Kawamura, N., Suzuki, M. & Ishikawa, T. (2001). *Nucl. Instrum. Methods*, A**467-468**, 686–689.